Sindland, C., V. Andersen, and M. Tangstad. 2026. Silicon Carbide Reactivity: Experimental study of the reaction between SiC and SiO gas. In *Silicon for the chemical and solar industry XVIII,* edited by M. Tangstad, H. Rong, A. Valderhaug, B. Andresen, H. Dalaker, and I. G. Page. Kristiansand, Norway, September 7–10, 2026. https://doi.org/10.55669/oa900813

Silicon Carbide Reactivity:
Experimental study of the reaction between SiC and SiO gas

C. Sindland[1,2], V. Andersen[1], and M. Tangstad[2]
[1]Elkem ASA, Norway, caroline.sindland@elkem.com. [2]Norwegian University of Science and Technology, Norway

Keywords: Silicon carbide, SiO gas, reactivity, reaction kinetics, experiments

Abstract – Silicon carbide (SiC) is an important intermediate material in silicon production. SiC is produced from reaction between carbon and SiO gas, and if it does not react further to silicon, it may accumulate in the furnace and affect material flow, gas flow and electrical conditions. This work presents a new experimental setup for studying the reaction between SiC and SiO gas in a resistance-heated furnace. SiO gas is generated in the lower part of the chamber and passes upward to react with SiC held at a higher temperature. The reactivity of three SiC materials was compared: β-SiC from charcoal, accumulated α-SiC from a silicon furnace, and α-SiC from an Acheson furnace. Degree of reaction was evaluated from mass change and silicon content measured by SEM and XRD.

The results show that the method can distinguish between SiC materials with different reactivity. Under the tested conditions, β-SiC from charcoal showed higher reactivity than accumulated α-SiC from a silicon furnace and α-SiC from an Acheson furnace. A simple diffusion-based model gave a reasonable fit to the data and BET analysis suggests that surface area may be important for the observed differences. The results indicate that SiC reactivity is in important factor when the overall efficiency of a furnace is considered.

1. INTRODUCTION

Silicon is produced by carbothermic reduction of quartz in a submerged arc furnace, through several reactions. In the hot lower part of the furnace, SiO gas is formed and may then react with carbon to form SiC or with SiC to form silicon, as illustrated in Figure 1.

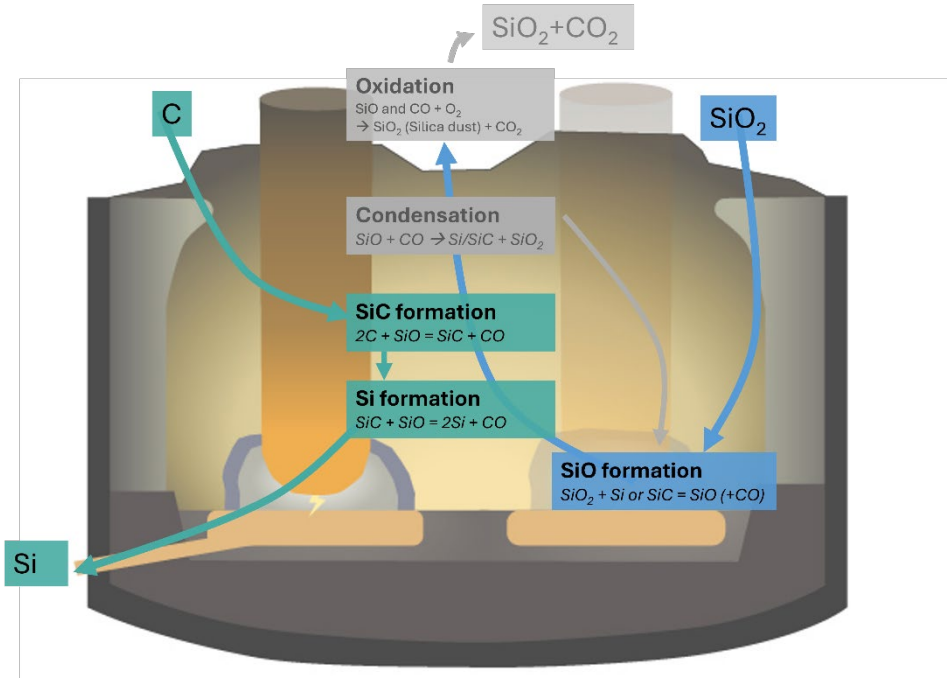

Figure 1: Illustration of the main reactions in a silicon furnace.

There should be a balance between SiC formation and SiC consumption. Accumulated SiC reduces the available reaction volume in the furnace and may also disturb electrical conditions (Haraldsson et al., 2024; Risinggård et al., 2022; Sindland et al., 2026; Tesfahunegn et al., 2018). While carbon reactivity towards SiO has been studied in detail (Lindstad et al.,2007; Myrhaug, 2003; Myrvågnes, 2008), there is limited published work on the reaction between SiC and SiO as described by Equation 1. In process models such as the two-zone model (Schei, Tuset and Tveit, 1998), this reaction is often assumed to reach equilibrium. In this work, we test whether SiC reactivity differs between materials and whether this difference can be measured experimentally.

$$SiC + SiO = 2Si + CO_{(g)} \qquad [1]$$

In the two-zone model (Schei, Tuset and Tveit, 1998), silicon formation from SiO and SiC takes place in the inner zone of the furnace. The partial pressure of SiO leaving the inner zone is described as the S-factor in this model. This factor is about 0.5 at 1970 °C if the reaction between SiC and SiO is significantly faster than the SiO formation rate, and it increases as the rate of SiO consumption decreases relative to SiO formation, as shown in Figure 2. The SiO leaving the inner zone must either react with carbon higher in the furnace or condense to maintain a high silicon yield. There must be a balance between SiC formation and SiC consumption over time to maintain stable operation, which implies that an increased S-factor will lead to increased condensation or formation of silica fume and thereby reduce yield. Condensation will move energy from the inner zone to the outer zone, since SiO formation is endothermic while condensation is exothermic, and it will form a highly viscous phase that prevents even gas and material flow, reducing overall efficiency. This makes SiC reactivity very relevant for process efficiency and stability by contributing to a low S-factor.

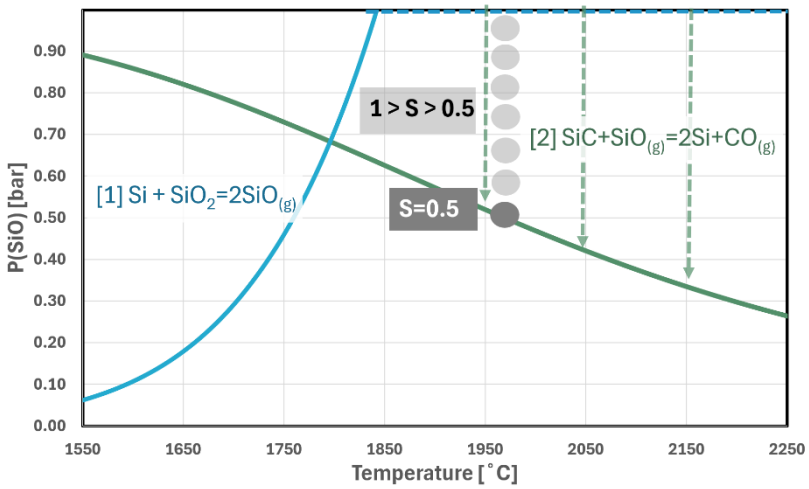

Figure 2: The equilibrium partial pressure of SiO for SiO formation [1] and silicon formation [2], given an activity of 1 for silicon. The dotted lines indicate the produced SiO pressure in the experimental setup of this paper and the driving force for silicon production at three temperatures. The figure illustrates how a lower rate of reaction [2] would increase the S-factor.

Silicon carbide (SiC) exists in several crystal structures, referred to as polytypes. In this work, β-SiC refers to the cubic 3C polytype, while α-SiC refers to the hexagonal and rhombohedral polytypes, which are commonly associated with higher formation temperatures (Jepps and Page, 1983). In silicon furnaces, β-SiC is typically formed first and may transform to α-SiC at higher temperatures (Jayakumari, 2020).

2. SiC reactivity test: Methodology and results

A method has been developed for testing relative SiC reactivity, and the setup has been used to compare β-SiC from charcoal, accumulated α-SiC from a silicon furnace, and α-SiC from an Acheson furnace. In this section, the setup and the basis for calculating degree of reaction are presented. Modelling of the SiC + SiO reaction rate based on these results is discussed in Section 3.

2.1 The SiC reactivity setup and raw materials

The SiC reactivity setup is illustrated in Figure 3. A total of 30 g of SiO granules are placed in a lower graphite crucible, while 10 g of SiC is placed in a perforated upper crucible. Because the lower part of the setup is colder than the upper part, SiO is generated below and passes upward to react with the hotter SiC. This design reduces premature condensation and allows the SiC to reach reaction temperature before significant SiO production starts.

Some SiO also reacts with graphite in the setup. This affects the CO content in the off-gas and is considered when interpreting the experiments and modelling the SiC + SiO reaction rate.

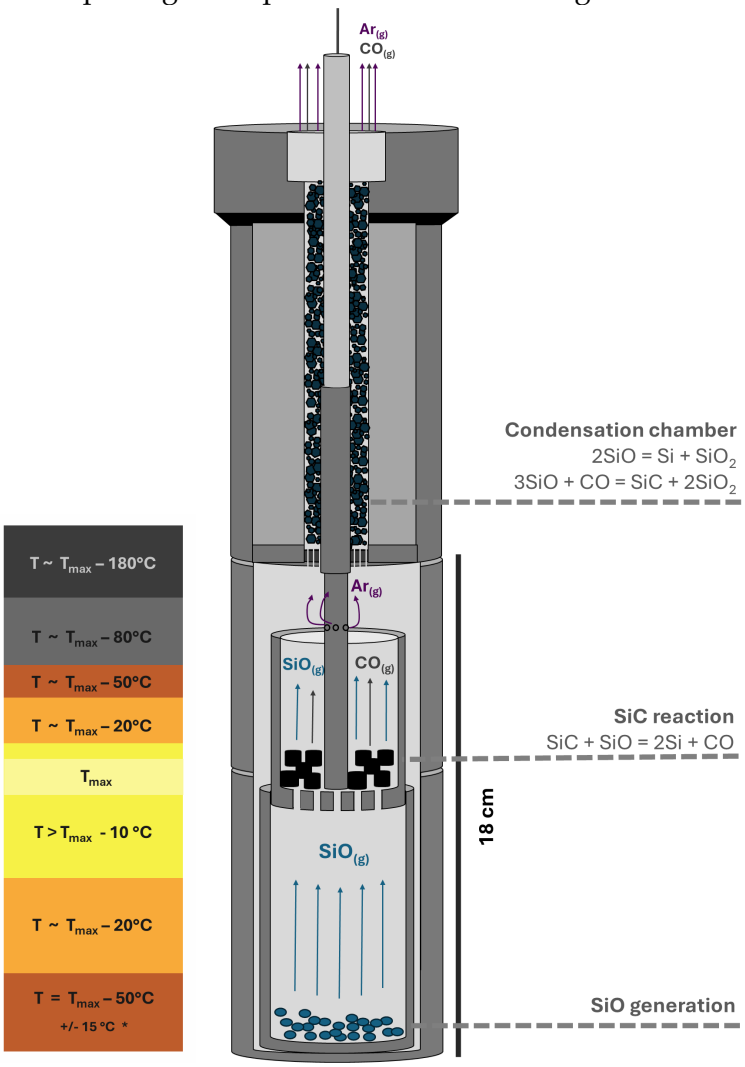

Figure 3: SiC reactivity setup with a lower chamber for SiO generation and an upper chamber for SiC reaction. The figure is adapted from Straum (2026).

Three types of SiC materials were tested: β-SiC from charcoal, accumulated α-SiC from a silicon furnace (same as investigated by Sindland et al., 2026), and α-SiC from an Acheson

furnace. The charcoal SiC was produced by calcining charcoal at 1200 °C for 20 minutes before exposing it to SiO gas for 1 h at 1800 °C. Before testing, the materials were crushed, sieved, and split into 10 g samples. The raw materials were analysed by scanning electron microscope (SEM) and X-ray diffraction (XRD) before reactivity testing.

Figure 4 shows the morphology of the three materials before reaction and their phase distribution before and after reaction with SiO, based on SEM images of cross section. The materials differ in morphology and porosity, and a clear increase in silicon content is observed after reaction. The silicon content, determined by SEM image analysis, and particle size of the raw materials is included in the figure.

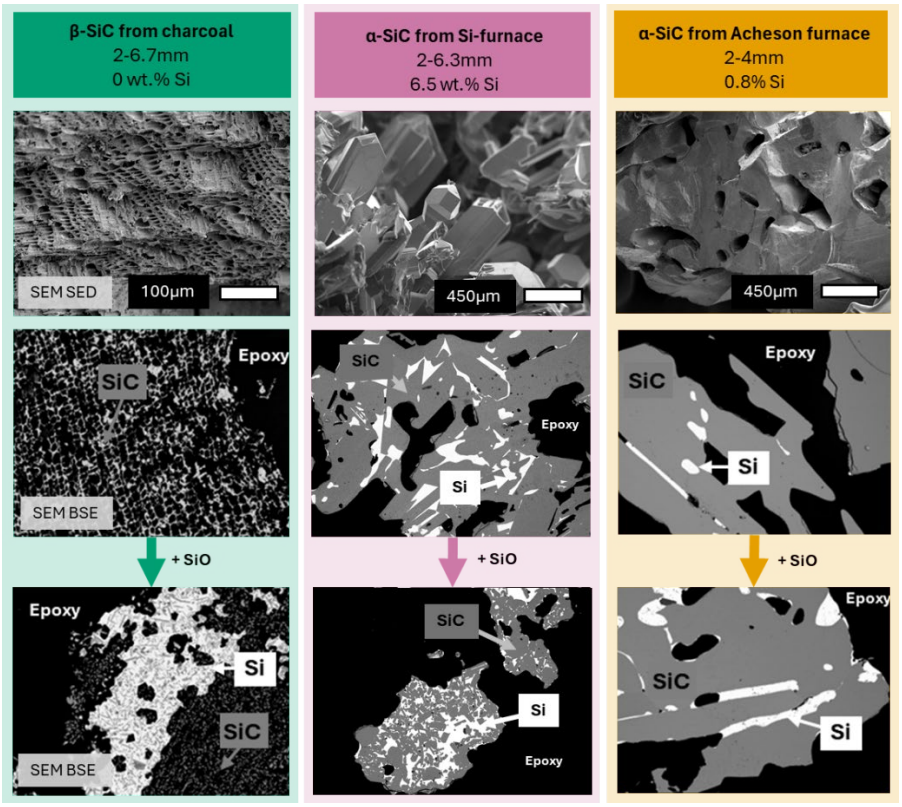

Figure 4: SEM images of the different SiC materials before and after reaction with SiO.

The materials were heated to temperatures from 1840 to 2140 °C and held for 5 to 60 minutes, as shown in Figure 5. CO in the off-gas reflects CO formation through both the SiO + SiC and SiO + C reactions, as well as CO consumption by condensation of SiO and CO. The CO content in the off-gas therefore cannot be used directly as a measure of SiC reactivity, in difference to the SINTEF SiO-reactivity test for carbon materials (Lindstad et al., 2007). The CO measurements are, however, useful for identifying when gas-phase reactions occur.

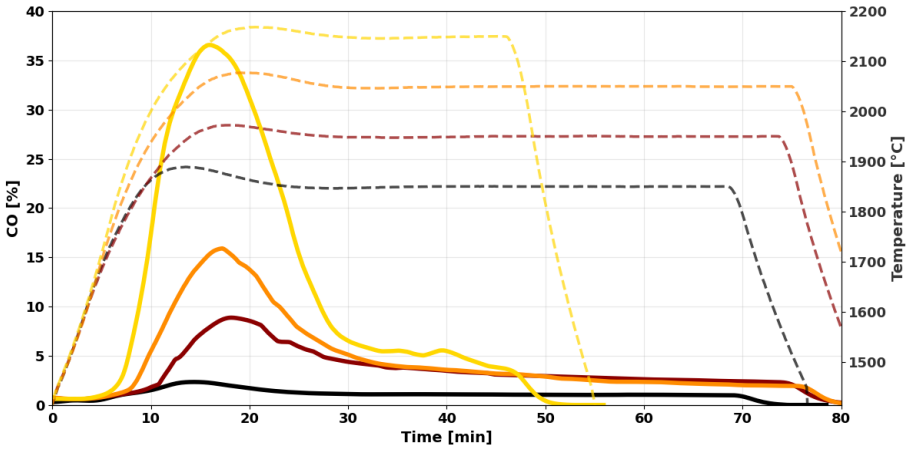

Figure 5: Heating program and CO evolution for typical experiments at four temperatures. CO concentration (%) in the off-gas is plotted as solid lines (left axis) while temperature is shown as dashed lines (right axis). The same colour is used for the corresponding CO and temperature curves.

Figure 6 shows that the SiO-generation data from Sindland and Tangstad (2020), Sindland (2026), and Kyaw (2024a and b) can all be described reasonably well by the same model structure proposed by Sindland (2020), $d\alpha/dt = A \cdot k \cdot \exp(-Q/RT)$, with relatively small deviations from the fitted curves within each dataset. The difference in reaction rates between the datasets of Sindland (2020) and Sindland (2026) is likely related to differences in available reaction area arising from the use of 1–8 mm particles and 2–4 mm granules, respectively. In particular, the external granule size cannot be directly compared with particle size, as the granules consist of finely distributed Si and SiO_2, resulting in a larger effective reaction area. However, the substantially higher reaction rates reported by Kyaw (2024a and b), from experiments where argon was purged through the SiO-forming chamber, suggest that gas flow conditions may also influence the observed SiO generation. Consequently, SiO generation should not be considered a function solely of temperature, time, and particle size, but also of material morphology and experimental design.

For the present study, all experiments were conducted using the same granule size fraction and gas flow conditions. Therefore, relative differences in SiC reactivity can be compared without accounting for variations in SiO generation. However, potential differences in SiO generation should be considered when experimental conditions are changed or when results are compared with data obtained using different experimental setups.

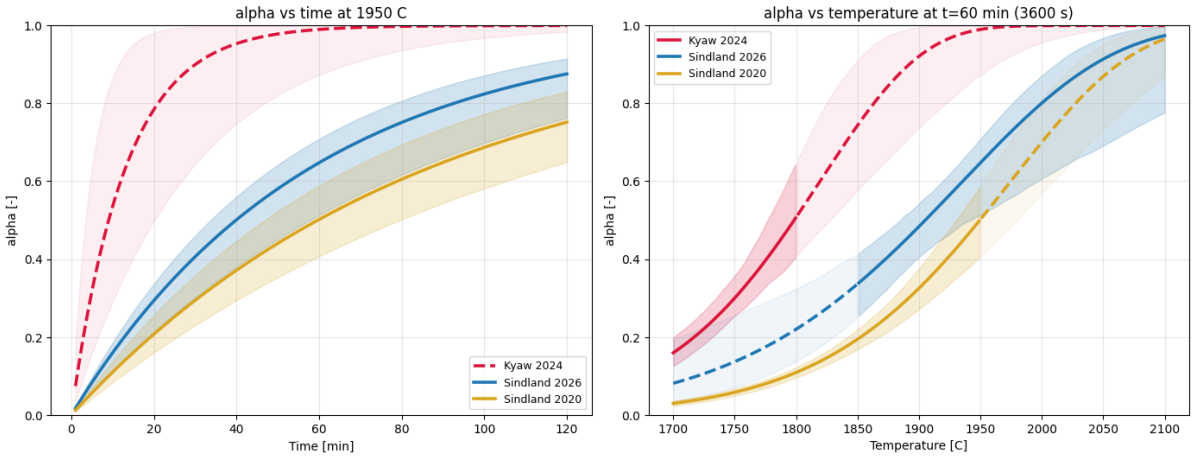

Figure 6: Modelled degree of reaction for the Si + SiO_2 = 2SiO reaction for three experimental setups using the equation proposed by Sindland (2020). Dashed lines indicate extrapolation beyond the measured temperature range. The shaded area represent the 95% confidence intervals.

2.2 Degree of reaction (SiC conversion to Si)

Degree of reaction is calculated as the amount of silicon carbide that has reacted, as described by Equation [2]. The initial and final amount of SiC ($SiC_{initial}$ and SiC_{final}) is given by the particle mass before and after the test ($m_{initial}$ and m_{final}) and their SiC content. The particles consist of SiC with some silicon, meaning that the SiC content can be calculated from the silicon content (%SiC = 100 - %Si).

$$\alpha = \frac{SiC_{initial} - SiC_{final}}{SiC_{inital}} = \frac{m_{initial} \cdot (100 - \%Si_{initial}) - m_{final} \cdot (100 - \%Si_{final})}{m_{initial} \cdot \%SiC} \qquad [2]$$

The silicon content was measured by XRD and SEM image analysis. For XRD, the material was milled and prepared for analysis on a Bruker D8 ADVANCE by back loading to reduce preferred orientation. Quantitative phase analysis was performed by Rietveld refinement in TOPAS v6. For SEM image analysis, approximately 10 grayscale images from each sample were segmented into epoxy, SiC, and silicon using fixed threshold values. A 3-point smoothed image was used to reduce misclassification caused by image resolution, and the bottom part of each image containing SEM parameters was excluded. A visualization of the process is included in Figure 7. The area fraction of silicon measured by SEM, relative to the combined Si and SiC content, was assumed to be equal to the volume fraction and was then converted to weight percent using the densities of Si and SiC.

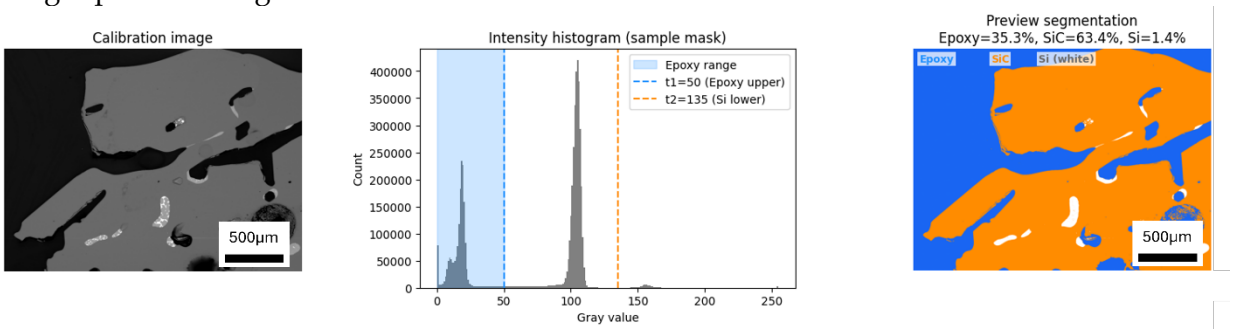

Figure 7: SEM image analysis method used to classify epoxy, SiC, and silicon from grayscale SEM images (50x).

A comparison of silicon content measured by XRD and SEM image analysis is presented in Figure 8. The two methods show the same main trend, but silicon content based on image analysis tends to be somewhat higher. The choice of SiC polytypes and parameters in the XRD refinement can influence the estimated silicon content, while for SEM image analysis there is uncertainty related to which particles are captured by the images. In the present work, the SEM results are used together with the mass change to estimate the degree of reaction.

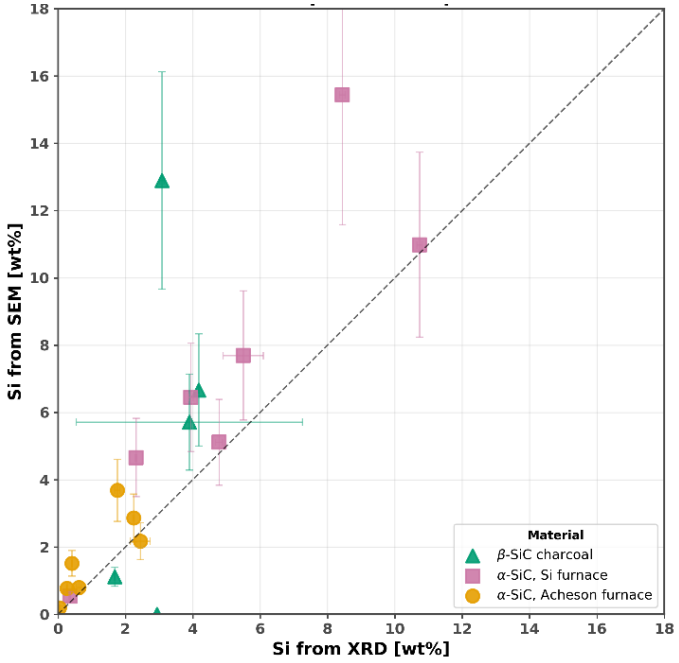

Figure 8: Silicon content determined by SEM image analysis and XRD.

Table I summarizes the experimental conditions and the calculated degree of reaction for the experiments used in the modelling.

Table I: Experimental conditions and degree of reaction for the experiments used in the modelling of SiC reactivity. *Negative degree of reaction is possible due to uncertainty in the measurement of silicon content.

Material	Run #	Temperature SiC [˚C]	Time [min]	SiC weight change [%]	Silicon after reaction [wt.%]	Degree of reaction (α)
β-SiC Charcoal	8	1940	60	+0.60	1.1	0.01
	17	2040	5	-1.11	5.7	0.10
	15	2040	60	+1.90	12.9	0.15
	19	2140	5	+8.96	6.7	0.12
α-SiC Si furnace	5	1840	60		0.54	
	7	1940	60	-1.70	5.1	0.00
	9	1940	60	-1.50	4.7	-0.01*
	14	2040	60	+2.00	7.7	0.00
	18	2090	30	-3.00	11.0	0.09
	12	2140	30	+3.01	15.4	0.10
α-SiC Acheson furnace	4	1840	60		0.2	
	6	1940	60	-1.20	2.2	0.03
	16	1990	60	+0.80	2.9	0.02
	10	2040	60	+0.90	3.7	0.03

Figure 9 shows CO content in the off-gas as a function of time for all experiments performed at 1940 °C. There is a large variation in the total amount of CO produced, and the amount of CO is not necessarily lower when there is no SiC in the system. This confirms that the CO measurements cannot be used as a measure of degree of reaction, as discussed previously.

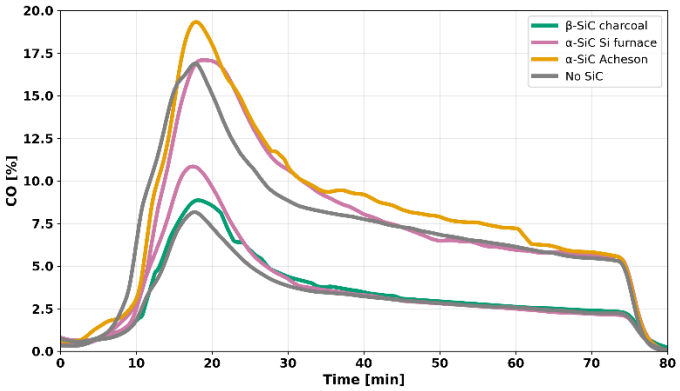

Figure 9: CO in the off-gas for all experiments at 1940 °C, including experiments without silicon carbide.

The silicon carbide produced from charcoal is initially β-SiC, while it transforms into α-SiC when exposed to temperatures above 2000 °C, as presented in Figure 10. Most of the results follow the trend where degree of transformation increases with temperature above 2000 °C, as discussed by Jayakumari (2020). However, the results at 2040 °C are unexpected regarding effect of time and more results are needed to indicate any clear trend and mechanism behind the transformation from β to α-SiC under exposure to SiO gas.

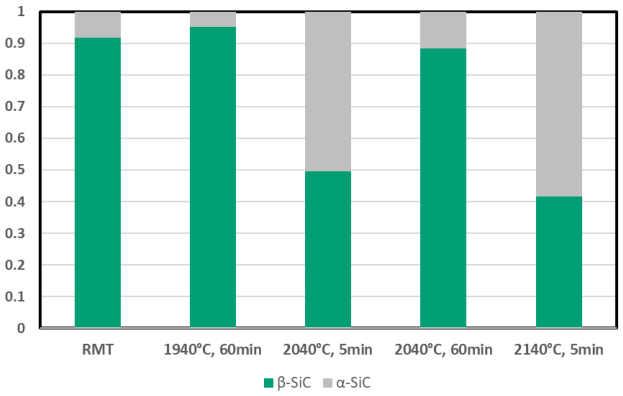

Figure 10: Content of β- and α-SiC in charcoal SiC before and after exposure to SiO gas at elevated temperatures.

3 Modelling of SiC reactivity

The purpose of the modelling is to describe how the degree of reaction depends on time and temperature, and to compare the relative reactivity of the tested SiC materials.

A simple diffusion-based expression (D1, Equation 3) was used as a framework to describe the dependence of the calculated degree of reaction on time and temperature (Khawam and Flanagan, 2006). The present dataset is limited, with only a few experiments for each material, and is therefore not sufficient to identify the controlling reaction mechanism or to validate one kinetic model over another. The model should consequently be regarded as a preliminary and comparative description of the data, rather than a mechanistic fit. Its purpose is to provide an initial basis for comparing apparent SiC reactivity between materials and for comparing the relative rate of the SiC + SiO reaction with other furnace reactions. More experiments are needed to determine whether the selected model form is physically representative.

$$\alpha = k_{material} \cdot \sqrt{t} \cdot \exp\left(-\frac{Q}{RT}\right) \qquad [3]$$

In this model, the degree of reaction (α) depends on time (t), temperature (T), activation energy (Q), the gas constant (R), and a material-specific mass transfer constant (k). Differences between the tested materials are therefore represented by different fitted values of k, listed in Table II. A comparison of modelled and measured degree of reaction is presented in Figure 11.

Table II: Constants for the diffusion-based model used to describe SiC reactivity.

Constant	Value	Unit
$k_{material}$ (α-SiC Si furnace)	$1.5 \cdot 10^9$	$1/s^{0.5}$
$k_{material}$ (α-SiC Acheson furnace)	$1.6 \cdot 10^9$	$1/s^{0.5}$
$k_{material}$ (β-SiC charcoal)	$4.1 \cdot 10^9$	$1/s^{0.5}$
Q	545	kJ/mol

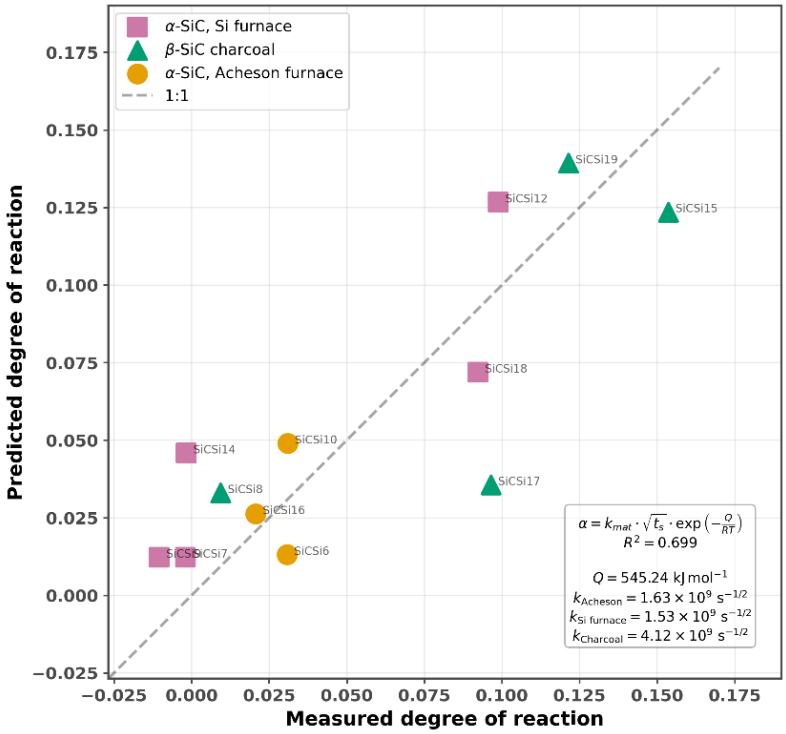

Figure 11: A comparison of predicted and measured degree of reaction for all experiments.

The fitted model gives an approximate description of the measured degree of reaction, but the limited number of data points and the uncertainty in the calculated degree of reaction mean that the fitted parameters should be interpreted with caution. Within these limitations, the results indicate that the apparent degree of reaction increases with temperature and time, as illustrated in Figures 12 and 13. The fitted material constants suggest that SiC from charcoal is more reactive than the two α-SiC materials under the tested conditions, while the two α-SiC materials behave similarly. The predicted reaction rate of charcoal SiC at 1950 °C is comparable to that of the α-SiC materials at about 2050 °C, illustrating the combined effect of material type and temperature.

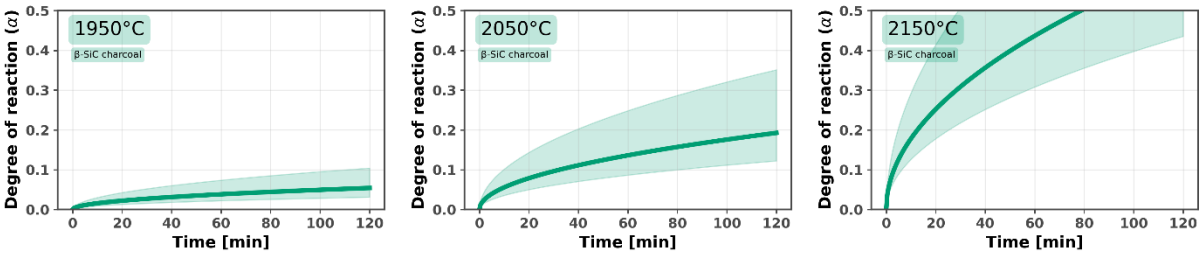

Figure 12: Model prediction of how the degree of reaction changes with time for β-SiC from charcoal at different temperatures. The shaded bands represent 50% confidence intervals from bootstrapping.

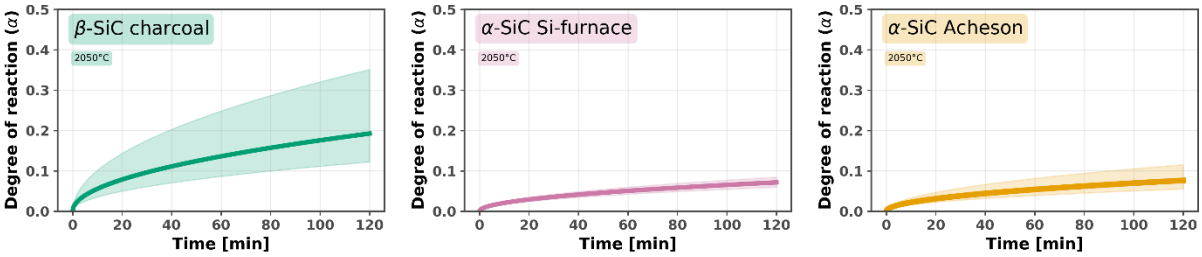

Figure 13: Model prediction of how the degree of reaction changes with time for the tested materials at 2050 °C. The shaded bands represent 50% confidence intervals from bootstrapping.

A comparison of BET surface area and the fitted material constant (mass transfer constant) in Figure 14 suggests that available surface area may be an important factor for SiC reactivity. The present results therefore indicate that surface area may be more important than polytype alone, but this cannot be concluded from the current dataset. This will be investigated further by testing α-SiC materials with higher specific surface area. We also aim to test various particle sizes in the future, as we expect that the rate of reaction increases with decreasing particle size.

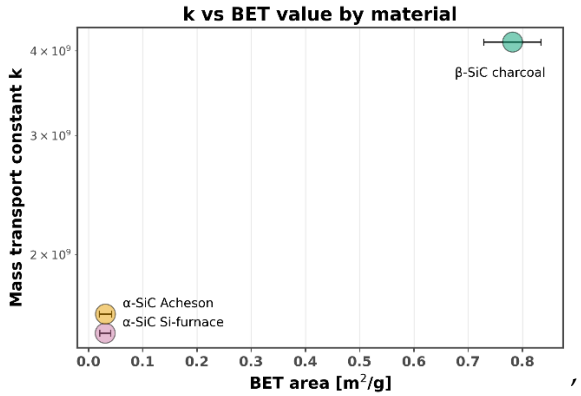

Figure 14: BET analysis of the three SiC materials before reactivity testing and their reactivity constants. The BET values for the α-SiC materials are outside the normal range for BET analysis due to their low specific area and should be considered approximate.

3.1 Comparison with other reactions and industrial implications

To explore the possible industrial relevance of the measured SiC reactivity, the newly developed model for the SiC + SiO = 2Si + CO reaction was combined with published models for SiO + 2C = SiC + CO, Si + SiO_2 = 2SiO, and SiC + $2SiO_2$ = 3SiO + CO (Myrhaug, 2003; Sindland, 2020; Tangstad, 2019). This makes it possible to compare the relative rates of important SiC-forming, SiO-forming, and Si-producing reactions under the same conditions.

Figure 15 compares the modelled degree of reaction as a function of time for several important furnace reactions at different temperatures and fixed particle sizes. The conversion of 4 mm

carbon particles to SiC is clearly the fastest reaction, which is consistent with furnace excavations showing SiC formation already in the upper part of the furnace (Ksiazek, Tangstad and Ringdalen, 2016). At 1850 °C, the SiO-forming reaction between 1–8 mm silicon and quartz proceeds only to a limited extent, whereas at 2050 °C significant SiO formation is predicted for both Si + SiO_2 and 3 mm SiC + SiO_2. In contrast, the predicted degree of reaction for SiC + SiO remains relatively low, indicating that SiC consumption may be slower than the competing SiO-forming reactions. The combined modelling should be regarded as indicative rather than conclusive, since some of the models were applied outside their original experimental ranges.

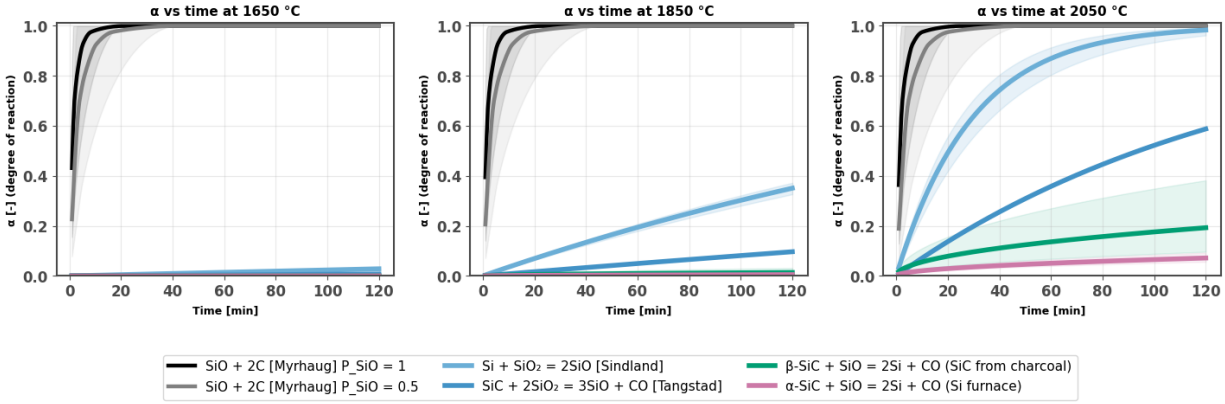

Figure 15: Modelled degree of reaction as a function of time for several furnace reactions at three temperatures.

The results indicate that SiC reactivity may be important for furnace operation. Accumulated SiC from a silicon furnace reacted more slowly with SiO than SiC produced from charcoal, and the combined modelling suggests that SiC consumption may be slower than some of the competing SiO-forming reactions. This means that low SiC reactivity may contribute to a higher SiO pressure leaving the inner zone, thereby increasing the need for SiO consumption by carbon or condensation higher in the furnace. If this consumption is insufficient, the probability of SiO loss as silica fume increases. The results therefore suggest that SiC reactivity should be considered alongside carbon reactivity in further discussion and modelling of furnace efficiency and yield.

4. CONCLUSIONS

The developed setup shows potential for comparing SiC reactivity of different materials under controlled conditions. The results indicate that β-SiC from charcoal reacts faster with SiO than the two tested α-SiC materials, although additional experiments are needed to confirm the trend and determine whether the fitted reaction model is physically representative. The results also suggest that specific surface area may contribute to the observed differences between the materials, but more data are needed before this can be concluded.

The comparison with published reaction models indicate that the SiC + SiO reaction is slower than several competing SiO-forming reactions, meaning that SiC reactivity is relevant for SiO consumption in the inner zone of the furnace. This means that SiC reactivity should be considered in further modelling and discussion of furnace operation.

5. ACKNOWLEDGEMENTS

The authors gratefully acknowledge the financial support from the Research Council of Norway (project number 354123) and Elkem ASA.

6. REFERENCES

Filsinger, D.H. and Bourrie, D.B., 1990. Silica to Silicon: Key Carbothermic Reactions and Kinetics. Journal of t*he American Ceramic Society*, 73, pp.1726–1732.

Haraldsson, H.V., Traustason, H., Tesfahunegn, Y.A., Tangstad M. and Sævarsdottir G., 2024. Modeling and Comparison Study of Industrial AC-Arcs. *Metallurgical and Materials Transactions B*, 55, pp.3750–3760.

Jayakumari, S., 2020. *Formation and Characterization of β- and α-Silicon Carbide Produced During Silicon/Ferrosilicon Process*. Doctoral theses at NTNU, 2020:252.

Jepps, N.W. and Page, T.F., 1983. Prog. Cryst. Growth Charact., 7, p.259.

Khawam, A. and Flanagan, D.R., 2006. Basics and applications of solid-state kinetics: A pharmaceutical perspective. *Journal of Pharmaceutical Sciences*, 95, pp.472–498.

Lindstad, T., Gaal, S., Hansen, S. and Prytz, S., 2007. Improved SINTEF SiO-reactivity test. In: *INFACON XI: Innovations in the Ferro Alloy Industry*, Vol. 1, pp. 414–423.

Ksiazek, M., Tangstad, M. and Ringdalen, E., 2016. Five furnaces five different stories. In: *Silicon for the chemical and solar industry XIII*, Kristiansand, Norway, 13 June 2016.

Kyaw, T.T. and Tangstad, M., 2024a. SiC formation in charcoal briquettes versus bulk material. In: *INFACON XVII*, Beijing, China, 13–22 September 2024.

Kyaw, T.T. and Tangstad, M., 2024b. Use of Agglomerates in Silicon Production. In: *Silicon for the Chemical and Solar Industry XVII*, Trondheim, September 2024.

Myrhaug, E.H., 2003. *Non-fossil reduction materials in the silicon process - properties and behaviour*. PhD thesis. Norwegian University of Science and Technology, Trondheim.

Myrvågnes, V., 2008. *Analyses and Characterization of Fossil Carbonaceous Materials for Silicon Production*. PhD thesis. Norwegian University of Science and Technology, Trondheim.

Risinggård, V.K., Sparta, M., Fromreide, M. and Halvorsen, S.A., 2022. Large electrode movements: Realistic electrical crater models. In: *Silicon for the Chemical and Solar Industry XVI*, Trondheim, Norway, 14–16 June 2022.

Schei, A., Tuset, J.K. and Tveit, H., 1998. *Production of High Silicon Alloys*. Trondheim: Tapir.

Sindland, C. and Tangstad, M., 2021. Production Rate of SiO Gas from Industrial Quartz and Silicon. *Metallurgical and Materials Transactions B*, 52B.

Sindland, C., Tangstad, M. and Andersen, V., 2026. Formation of α-SiC in the Low-Temperature Zone of Silicon Furnaces. *JOM*.

Straum, I., Behaviour of Quartz–Charcoal Agglomerates in Silicon Production 2026. *Master thesis*. June 2026.

Tangstad, M., Safarian, J., Bao, S., Ringdalen, E. and Valderhaug, A., 2019. Effect of Different SiO2 Polymorphs on the Reaction Between SiO2 and SiC in Si Production. *Aspects in Mining & Mineral Science*, 3, p.2.

Tesfahunegn, Y.A., Magnusson, T., Tangstad, M. and Saevarsdottir, G., 2018. Effect of Carbide Configuration on the Current Distribution in Submerged Arc Furnaces for Silicon Production—A Modelling Approach. In: Nastac, L., Pericleous, K., Sabau, A., Zhang, L., Thomas, B. (eds) CFD Modeling and Simulation in Materials Processing 2018. TMS 2018. The Minerals, Metals & Materials Series. Springer, Cham. https://doi.org/10.1007/978-3-319-72059-3_17

Caroline Sindland

Industrial PhD candidate and Research Engineer, Elkem ASA

Caroline Sindland is an Industrial PhD candidate and Research Engineer at Elkem ASA. She began her career as an apprentice in chemical analysis at Elkem, before completing an MSc in Materials Science and Engineering at NTNU. She later returned to Elkem as a Process Engineer. Since January 2025, she has been pursuing an industrial PhD on silicon carbide behaviour in silicon furnaces, in collaboration with NTNU.